Science of Sintering, **50** (2018) 193-203

doi:https://doi.org/10.2298/SOS1802193M

UDK 620.181.4; 531.3; 661.112.3

Non-Isothermal Crystallization of Lithium Germanophosphate Glass Studied by Different Kinetic Methods

Srđan D. Matijašević[1*)], Snežana R. Grujić[2], Vladimir S. Topalović[1], Jelena D. Nikolić[1], Sonja V. Smiljanić[2], Nebojša J. Labus[3], Veljko V. Savić[1]

[1]Institute for Technology of Nuclear and other Mineral Raw Materials (ITNMS), 86 Franchet d Esperey St., 11000 Belgrade, Serbia

[2]Faculty of Technology and Metallurgy, University of Belgrade, 4 Karnegijeva St., 11000 Belgrade, Serbia

[3]Institute of Technical Sciences of SASA, Knez-Mihailova 35/IV St., 11000 Belgrade, Serbia

Abstract:

Crystallization kinetics of $22.5Li_2O•10Al_2O_3•30GeO_2•37.5P_2O_5$ (mol%) glass was studied under non-isothermal condition using the differential thermal analysis (DTA). The study was performed by using the first crystallization peak temperature (T_{p1}) which belongs to the precipitation of $LiGe_2(PO_4)_3$ phase in the glass. The activation energy of glass crystallization (E_a) was determined using different isokinetic methods. The dependence of E_a on the degree of glass-crystal transformation (α) was studied using model-free isoconversional linear integral KAS (Kissinger–Akahira–Sunose) and FWO (Flynn–Wall–Ozawa) methods. It was shown that the E_a varies with α and hence with temperature and consequently the glass/crystal transformation can be described as a complex process involving different mechanisms of nucleation and growth.

Keywords*: Lithium germanophosphate glass; Crystallization kinetics; DTA; nucleation.*

1. Introduction

Lithium germanophosphate glasses have recently emerged as multipurpose materials and have drawn great attention because of their potential applications in various solid state devices [1, 2]. By crystallization of some glasses from the system Li_2O-Al_2O_3-GeO_2-P_2O_5, the $LiGe_2(PO_4)_3$ phase which belongs to the solid solutions with general formula of $Li_{1+x}M_xGe_{2-x}(PO_4)_3$ (M=Al, V or Cr) is formed. This family of the crystalline phosphates is often referred to as NASICON-type materials [3, 4]. It is important to know the crystallization behavior of the parent lithium phosphate glass in order to define technological parameters for fabrication of these structured materials. The crystallization kinetics of glasses can be successfully studied using the DTA or DSC techniques and for evaluation of the kinetic parameters of crystallization several methods classified as isokinetic and isoconversional (model-free) are used. Isokinetic methods assume the transformation mechanism to be same throughout the temperature or time range and allow calculating single values of the kinetic parameters such

*) **Corresponding author:** s.matijasevic@itnms.ac.rs

as the activation energy [5-11]. On the other hand, isoconversional methods assume the transformation mechanism at a constant degree of conversion as a function of temperature and provide kinetic parameters varying with the degree of conversion, α.
The determination of the dependence of E_a on α can give useful information about complexity of transformation mechanism and kinetics scheme of the process as well [12-18].

In this work the results of non-isothermal crystallization of $22.5Li_2O•10Al_2O_3•30 GeO_2•37.5 P_2O_5$ (mol%) glass performed by DTA were reported and discussed.

The kinetic parameters of crystallization were calculated using different methods and the dependence of the activation energy of crystallization (E_a) on the volume fraction crystallized (α) was studied using isoconversional linear integral KAS (Kissinger–Akahira–Sunose) [12] and FWO (Flynn–Wall–Ozawa) methods [14, 16].

2. Experimental

2.1. Glass preparation

The parent glass was prepared by melting a homogeneous mixture of reagent-grade Li_2CO_3, Al_2O_3, GeO_2 and $(NH)_2HPO_4$ in a covered platinum crucible. The melting was performed in an electric furnace BLF 17/3 at T=1400 °C for t=0.5 h. The melts were cast on a steel plate and cooled in air. The obtained glass samples were transparent, without visible residual gas bubbles. XRD analysis confirmed an amorphous structure of the sample. The chemical composition was determined using spectrophotometer AAS PERKIN ELMER Analyst 300.

2.2. DTA experiments

The experiments under non-isothermal conditions were performed using a DTA-Netzsch STA 409 EP device and Al_2O_3 powder as the reference material. The powder glass samples were prepared by grinding the bulk sample in an agate mortar and then sieving it on standard sieves up to the grain size of 0.50-0.65 mm. In the experiments, constant weights (100 mg) of the powdered glass samples were heated at different rates (β) of 5, 10, 15 and 20 °C/min from 20 °C to 1150 °C.

3. Results and Discussion

3.1. Thermal analysis (DTA)

In Fig. 1 DTA curves of the powdered glass sample recorded at heating rates β of 5, 10, 15 and 20 °C/min from 20 °C to 1150 °C are shown. The glass transition temperature T_g is determined as an inflexion point on curves (510, 517, 522, 527 °C). T_x is onset crystallization temperature (620, 630, 640, 645 °C). Two exothermal crystallization peaks T_{p1} (648, 658, 665, 671°C) and T_{p2} and endothermal one, T_m (1053, 1074, 1085, 1092 °C) representing the melting of sample were revealed. It is evident that the peak temperatures increase with increasing β. As revealed previously the peak T_{p1} belongs to the precipitation of $LiGe_2(PO_4)_3$ crystalline phase. The contribution of ~ 98 vol% of this phase in the crystallized glass was determined [19].

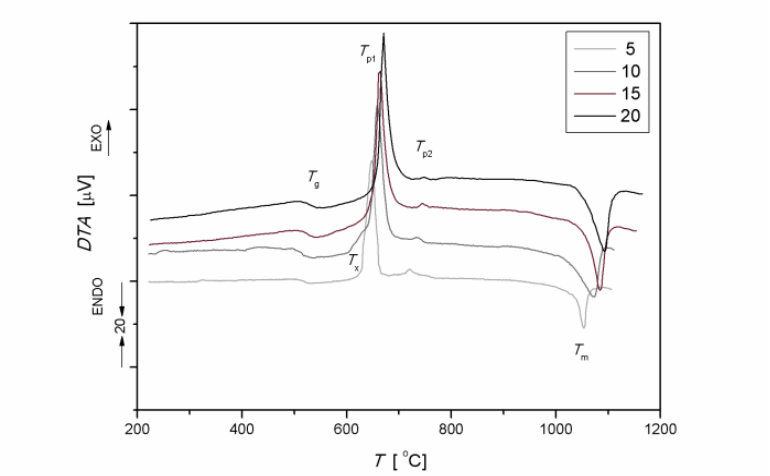

Fig. 1. DTA curves for glass powder sample recorded at different heating rates β.

The existence of correlation between glass forming ability (GFA) and glass stability (GS) under heating was established. Among several parameters for glass stability (GS) assessment, the Hruby parameter (K_H), is most frequently used [20, 21]:

$$K_H = \frac{T_x - T_g}{T_m - T_x} \quad (1)$$

This parameter correlates well with GFA for oxide glasses and thus can be commonly employed as a reliable and precise glass-forming criterion. According to Hruby criterion, the higher the value of K_H for a certain glass, the higher its stability against crystallization is. Based on DTA (Fig. 1), an average value of K_H = 0.26 was calculated. This indicates low glass stability against crystallization and consequently its low glass forming ability (GFA). The value of reduced glass transition temperature $T_{rg}= T_g/T_m < 0.58$ suggests that this glass has volume (homogenous) nucleation [22].

3.2. Non-isothermal crystallization kinetics

To study the kinetics of glass crystallization under non-isothermal condition the isokinetic and isoconversional methods were employed.

The isoconversional methods assume that kinetic parameters vary with the degree of conversion α, unlike isokinetic models which allows us to calculate a single value of the kinetic parameters. Most of the isokinetics models are based on Kolmogorov-Johnson-Mehl-Avrami (KJMA) relation where the degree of transformation α is given by [16, 23]:

$$\alpha = 1 - \exp\left[(Kt)^n\right] \quad (2)$$

where n is dimensionless Avrami constant related to nucleation and growth mechanism and K is reaction rate constant usually assigned an Arrhenian temperature dependence:

$$K = K_o \exp(-E/RT) \quad (3)$$

where E is the effective activation energy of the overall crystallization process, K_o (s^{-1}) is the pre-exponential (frequency) factor and R is the universal gas constant.

Following the method for analysis of non-isothermal crystallization data suggested by Matusita and Sakka, the kinetic parameters of crystallization can be determined using modified Kissinger equation [6, 24]:

$$\ln\frac{\beta^n}{T_p^2} = -\frac{m \cdot E_{a,m}}{R \cdot T_p} + const. \quad (4)$$

where n - is the Avrami parameter which indicates the crystallization mode and m is a numerical factor which depends on the dimensionality of crystal growth, β-heating rate, T_p-crystallization peak temperature. The value of activation energy E_a - is obtained from the ratio $\ln(\beta^n/T_p^2)$ *vs*. $1/T_p$ using the corresponding values for n and m.

To determine the parameter n, the Ozawa equation is used [9].

$$\left.\frac{\partial \ln(-\ln(1-a))}{\partial \ln \beta}\right|_T = -n \quad (5)$$

In Fig. 2, the plot of log [−ln(1 − α)] versus log (β) is shown, where α is the degree of glass - crystal transformation at four fixed different temperatures. The fraction of crystals (α), was obtained from the ratio $\alpha = A/A_o$ where A represents the peak area at the chosen temperature, while A_o is the total area of the corresponding DTA peak. The values of Avrami parameter n have been determined from the slopes of straight lines (Fig. 2). It is clear from the figure that n is temperature independent T and hence an average value of n can be calculated. The average value of n = (3.93 ± 0.48) is close to 4.

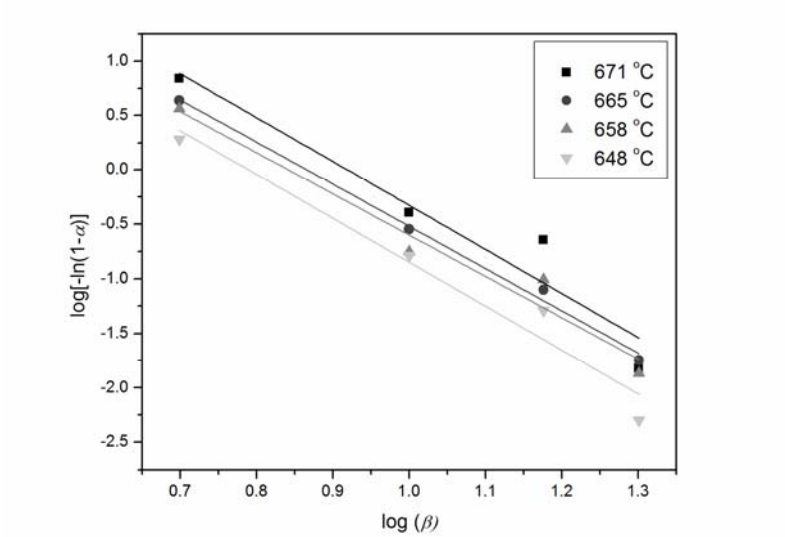

Fig. 2. log[−ln(1 − α)] against log (β) at different temperatures T [°C].

From Fig. 2 it can be seen that the plots are hardly found to be linear (esp. 648 and 671°C). In case of the present crystallization data the KJMA model can be questionable - note the positive asymmetry of the peaks (Fig.1 and Fig. 4), so the methodology for determination of n can be put up for discussion. There are a plenty of papers dealing with the capability to study the crystallization kinetics with the Matusita-Saka and Ozawa method [9]. Most of the times different mechanisms have been taking place during crystallization thus at the same temperature value different degrees of crystallization are connected with different mechanisms. So, it is not possible to take accepTab. linear plots. The relation proposed by Augis and Bennett [10] can be also used for determination of E_a:

$$\ln\left[\frac{\beta}{T_p - T_x}\right] \cong -\frac{E_a}{RT_p} + \ln K_0 \quad (6)$$

where T_x is crystallization temperature onset. The plot $\ln\left[\frac{\beta}{T_p - T_x}\right]$ vs. $1/T_p$ is shown in Fig. 3. From the slope of the line E_{aAB} = (471.02±28.80) kJ mol^{-1} was calculated.

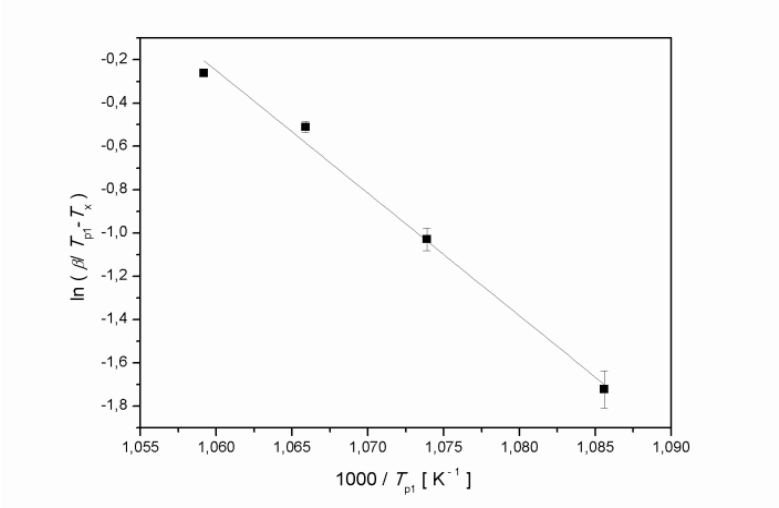

Fig. 3. The plot $\ln\left[\frac{\beta}{T_p - T_x}\right]$ vs. $1000/T_p$.

A method suggested by Gao and Wang [25] uses the following expressions derived from the Kolmogorov-Johnson-Mehl-Avrami (KJMA) equation [22] to determine E_a:

$$\ln\left[\frac{d\alpha}{dt}\right] \cong -\frac{E_a}{RT_p} + const. \quad (7)$$

where $(d\alpha/dt)_p$ is the rate of volume fraction crystallized at the peak of crystallization temperature T_p, which is proportional to exothermic peak height. In Fig. 4, the dependence of $(d\alpha/dt)$ on temperature at different heating rates is shown. It is clear from the Fig.4 that the peak height increases and shifts towards higher temperatures with the increase in heating rate. This is due to the fact that the rate of crystallization increases and crystallization shifts towards higher temperatures as well as heating rate β increase from 5 °C/min to 20 °C/min, i.e. more volume fraction is crystallized in a smaller time compared to the low heating rate fraction.

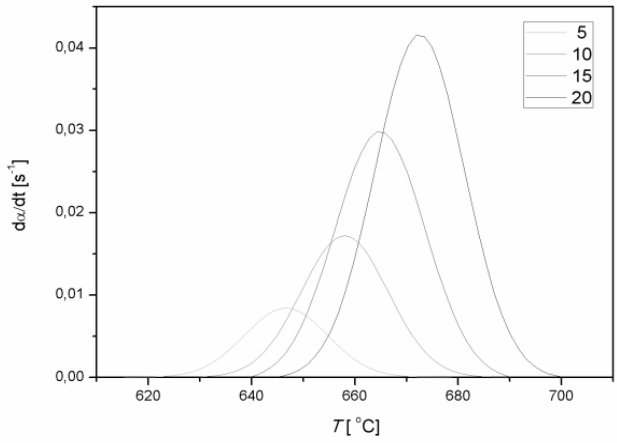

Fig. 4. $(d\alpha/dt)_p$ vs. T at different heating rates 5-20 °C/min.

The activation energy of crystallization can be determined from the plot $\ln\left[\frac{d\alpha}{dt}\right]$ vs. $1/T_p$, Fig. 5. From the slope of the straight line the activation energy of crystallization (E_{aGW}) = (515.12 ± 25.67) kJ mol^{-1} was calculated.

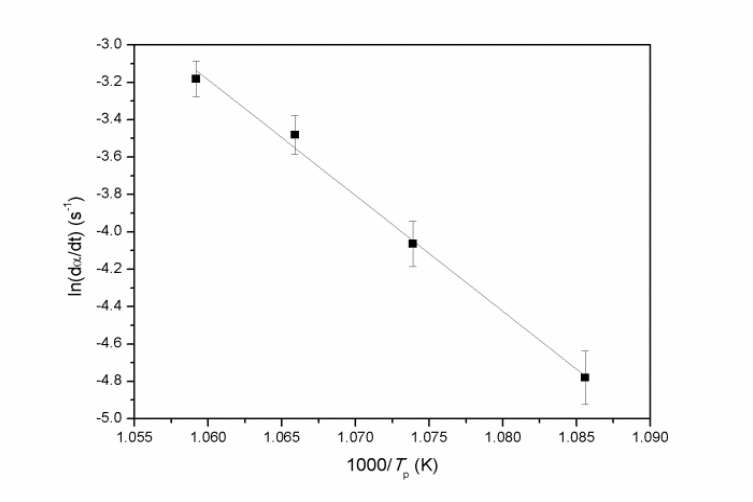

Fig. 5. $\ln\left[\frac{d\alpha}{dt}\right]$ vs. $1000/T_p$.

The activation energy of crystallization E_a was determined using the Kissinger equations [15]:

$$\ln\frac{\beta}{T_p^2} = -\frac{E_a}{R\cdot T_p} + const. \quad (8)$$

The values of E_{aK}= (440.21 ± 13.52) kJ mol^{-1} for Kissinger was determined from dependencies $\ln(\beta/T_p^2)$ vs. $1/T_p$ showed in Fig. 6. The activation energies of glass crystallization (E_a) determined by different methods are listed in Tab. I.

Tab. I Activation energies of glass crystallization (E_a) calculated by different methods.

Methods	E_a (KJ mol^{-1})
Augis and Bennett (Eq.6)	471.02±28.80
Gao and Wang (Eq.7)	515.12± 25.56
Kissinger (Eq.8)	440.21±13.52

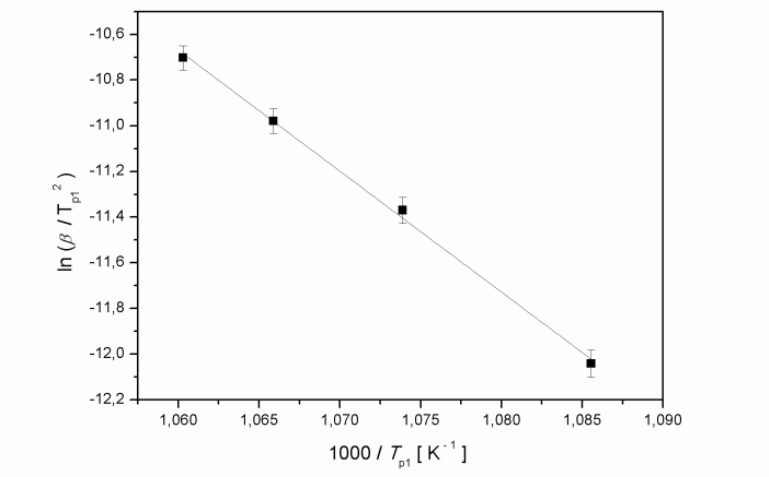

Fig. 6. $\ln(\beta/T_p^2)$ vs. $1000/T_p$.

It has been noted that the values of the activation energies of crystallization calculated by Augis & Bennett and Gao & Wang methods are higher than ones obtained by Kissinger. A certain difference has been observed in the values of E_a evaluated by different formulations. From Tab. I it is obvious that the accuracy of the calculation of E_a with the different methods is not accepTab. (values from 440 to 515 KJ/mol).

Unlike to isokinetic methods where the kinetic parameters of the process are assumed to be constant with respect to time and temperature, the isoconversional methods assume the transformation mechanism at constant degree of conversion as a function of temperature and provide the kinetic parameters that are varying with the degree of conversion, α. The dependence E_a on the degree of glass-crystal transformation α, should reflect to the change of nucleation and growth behavior during the crystallization process of glass. The isoconversional methods are based on the basic kinetic equation [16]:

$$\frac{d\alpha}{dT} = k(T)f(a) \tag{9}$$

where $k(T)$ is the rate constant as given by Eq. (3) and $f(\alpha)$ is the reaction model. By integrating Eq. (3), the integral form of the reaction model can be obtained as follows:

$$g(\alpha) = \int_0^{\alpha} [f(\alpha)]^{-1} d\alpha = \frac{k_0}{\beta} \int_0^{T} \exp\left(-\frac{E}{RT}\right) dT \tag{10}$$

Various approximations in the different isoconversional model proposed for determination of the kinetic parameters of glass crystallization were applied in order to simplify the temperature integral in Eq. (10).

To determine the activation energy of crystallization of this glass as a function of the fraction of crystallization, $E_a(\alpha)$, the Kissinger–Akahira–Sunose (KAS) and the Flynn–Wall–Ozawa (FWO) integral isoconversional methods for non-isothermal kinetic analysis were employed. For α = const., the apparent activation energy $E_a(\alpha)$ is determined by FWO (Eq. 11) and KAS (Eq. 12) relations [12, 14]:

$$\ln \beta = \ln\left(\frac{A_a E_{a,\alpha}}{R g(\alpha)}\right) - 5.331 - 1.052\frac{E_{a,\alpha}}{RT_\alpha} \tag{11}$$

$$\ln \frac{\beta}{T_a^{\,2}} = \ln\left(\frac{A_a R}{E_{a,\alpha} g(\alpha)}\right) - \frac{E_{a,\alpha}}{RT_\alpha} \tag{12}$$

where β is the heating rate, A_a is the apparent pre-exponent factor, E_a is the apparent activation energy, R is the gas constant, $g(\alpha)$ is the integral form of the reaction model and T is the temperature. The methods assume the conversion function $g(\alpha)$ to be constant for all values of conversion α at different heating rates β.

For α = const., the plots of ln β vs. $1/T_a$ (FWO) and ln ($\beta/T^2\alpha$) vs. $1/T_a$ (KAS), obtained from DTA curves recorded at several heating rates, should be straight lines. The apparent activation energies E_a (α) can be determined from the slopes of the lines. In Fig. 7, the volume fraction crystallized (α) as a function of temperature T at different heating rates β is shown. A systematic shift in α to higher temperature with an increase in heating rate β can be observed from this figure. Based on this curves obtained for the crystallized fraction in the range $0.1 \leq \alpha \leq 1$, E_a were calculated using Eq. 11 and 12.

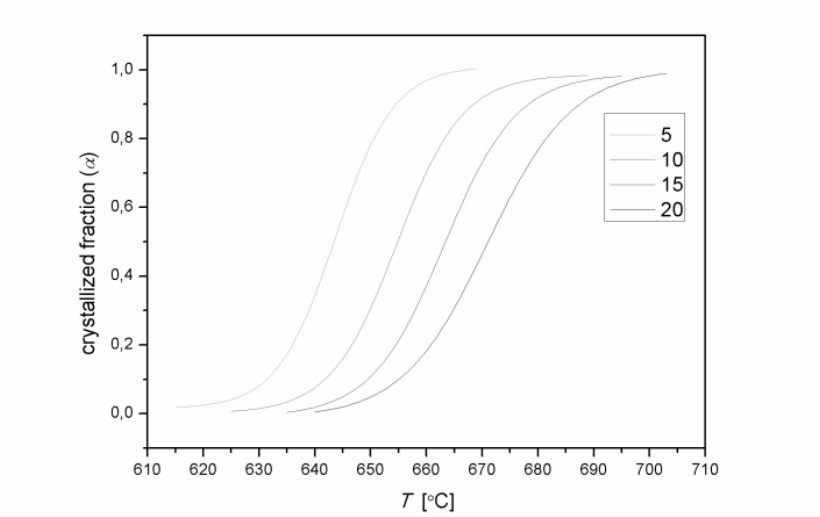

Fig. 7. Crystallized fraction (α) vs. temperature at different heating rates β.

The dependence of E_a on the crystallized fraction α is shown in Fig. 8. As may be seen in Fig. 8, the values of activation energies E_a strongly depend on α showing similar variation for both methods employed, the E_a decreased in all range of α. The average values of E_a = (347.62 ± 16.88) kJ mol^{-1} for FWO and E_a = (332.59 ±1 6.58) kJ mol^{-1} for KAS methods are in good agreement, but these values are significantly different from the ones determined by isokinetic methods (Tab. I).

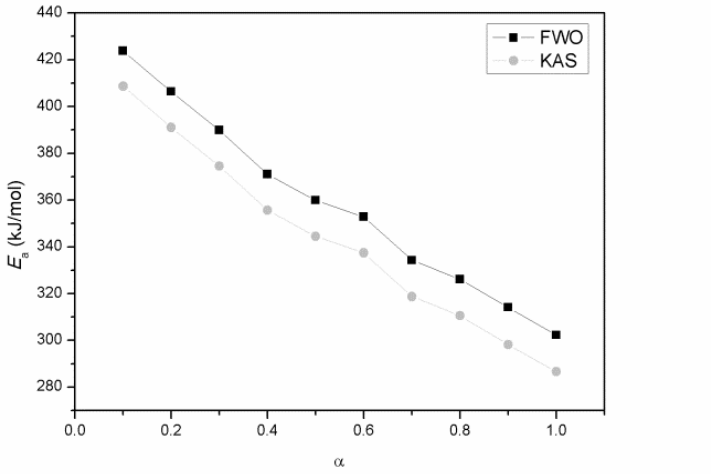

Fig. 8. The dependence of E_a on α using FWO and KAS methods.

According to ICTAC recommendations there is no need to use different methods for the calculation of activation energy [26]. From the presented methods only one isoconversional method must be valid. The activation energies of glass crystallization (E_a) determined by KAS and WFO methods are listed in Tab. II.

Tab. II Activation energies of glass crystallization (E_a) calculated by KAS and WFO methods.

Methods	E_a **(KJ mol^{-1})**
WFO (Eq.11)	347.62±16.88
KAS (Eq.12)	332.59±16.58

From Tab. II it is clear that the values of the activation energies of crystallization calculated by isoconversional methods are in a good accordance.

As reported earlier by Vyazovkin [27], the existence of the variation of activation energy (E_a) with the degree of crystallization (α), and hence with temperature, can give the information about complexity of the transformation mechanism and kinetics scheme of the process as well. The crystallization process is generally determined by nucleation and growth, which are very likely to have different activation energies. Three main nucleation mechanisms described as site saturation, continuous nucleation and mixed one can operate during crystallization. Growth kinetics can be controlled by interface reaction (crystal-melt interface) or diffusion. As these processes are in series, the total transformation kinetics will be primarily determined by slower process [28, 29]. Also, it is possible that different growth mechanisms are operating at different degree of crystallization leading to temperature-dependent activation energy [30-33]. Consequently, for this glass a strong variation of E_a on the degree of transformation (α), (Fig. 8) indicates that the glass/crystall transformation cannot be described as a simple single-step process. The existence of different kinetic mechanisms during crystallization of the studied sample is supported from the dependence of E_a, presented in Fig. 8.

It has been considered that during heating of this glass a complex crystallization process occurs where different mechanisms of nucleation and crystal growth are involved. Because these two mechanisms are likely to have different activation energies, the effective activation energy of the transformation will vary with α if nucleation and crystal growth aren't independent. This interpretation is based on the nucleation theory proposed by Turnbull and Fisher [34-36].

Large-scale lithium germanophosphate glass-ceramic with homogeneous ion conducting properties is difficult to fabricate, which limits its use in rechargeable lithium-ion batteries. Accordingly, volume crystallization is a significant finding, as it enables controlling the glass-ceramic microstructure. Recently, the volume crystallization mechanism and spherical growth morphology of $LiGe_2(PO_4)_3$ crystals has been determined also for a stoichiometric glass with the composition $Li_{1.5}$ $Al_{0.5}$ $Ge_{1.5}(PO4)_3$ [37, 38]. Taking in consideration the variation of E_a, it can be concluded that at early stage of crystallization the growth of nuclei is controlled by interface reaction. For further steps of crystallization the effect of volume controlled growth of crystals can be considered.

4. Conclusion

The crystallization process of $22.5Li_2O•10Al_2O_3•30GeO_2•37.5P_2O_5$ mol% glass was investigated under non-isothermal condition using DTA technique. Different isokinetic models were employed for determination of the kinetic parameters of glass crystallization, E_a. By using isoconversional KAS (Kissinger–Akahira–Sunose) and FWO (Flynn–Wall–Ozawa) methods a strong dependence of E_a on the degree of crystallization α and hence on temperature was detected. According to the experimental data obtained a complex transformation process governed by nucleation and diffusion mechanisms is suggested. The present study shows that for the complete description of glass crystallization kinetics a combined isokinetic and isoconversional non-isothermal analysis supported with microstructural data of the crystallized glass is necessary.

Acknowledgements

The authors are grateful to the Ministry of Education and Science, Republic of the Serbia for financial support (Projects 34001 and 172004).

5. References

1. K. Arbi, M. Ayadi-Trabelsi, J. Sanz, J. Mater. Chem., 12 (2002) 2985-2990.
2. C. Masquelier, Nat. Mater., 10 (2011) 649-650.
3. N. Anantharamulu, K. K. Rao, G. Rambabu, B. V. Kumar, V. Radha, M. Vithal, J. Mater. Sci., 46 (2011) 2821-2837.
4. C. Cao, Z. Li, X. L. Wang, X. Zhao, W. Q. Han, Front. Energy Res., 2 (2014) 1-10.
5. J. Šestak, Thermochim. Acta, 280-281 (1996) 175-190.
6. X. J. Xu, C. S. Ray., D. E. Day, J. Am. Ceram. Soc., 74 (5) (1991) 909-914.
7. H. E. Kissinger, Anal. Chem., 29 (1959) 1702-1706.
8. K. Matusita, S. Sakka, J. Non-Cryst. Solids, 38-39 (1980) 741-746.
9. T. Ozawa, J. Therm. Anal., 9 (1976) 369-373.
10. J. A. Augis, J. E. Bennett, J. Therm. Anal., 13 (1978) 283-292.
11. S. Vyazovkin, Isoconversional kinetics of thermaly stimulated processes, Springer Inter. Publishing, Switzerland, 2015.
12. T. Akahira, T. Sunose, Res. Report Chiba Inst. Technol. (Sci. Technol.), 16 (1971) 22-31.
13. H. L. Friedman, J. Polym. Sci., Part C6, (1964) 183-195.
14. J. H. Flynn, L. A. Wall, J. Res. Natl. Bur. Standards A. Phys. Chem., 70A (1966) 487-523.
15. S. Vyazovkin, J. Comput. Chem., 22 (2001) 178-183.
16. K. N. Lad, R.T. Savalia , A. Pratap, G.K. Dey, S. Banerjeeb,Thermochim. Acta, 473 (2008) 74-80.
17. J. Šestak, J. Malek, Solid State Ionics, 65 (1998) 245-254.
18. J. Farjas, P. Roura, ALChe J., 54 (2008) 2145-2154.
19. S. Matijašević, Crystallization behaviour of multicomponent germanate glasses, Doctoral dissertation, TMF, University of Belgrade, 2012. https://fedorabg.bg.ac.rs/fedora/get/o:6494/bdef:Content/get
20. A. Hruby, Czech. J. Phys., 22 (11) (1972) 1187-1192.
21. A. Kozmidis-Petrovic, J. Šestak, J. Therm. Anal. Calorim., 110 (2) (2012) 997-1004.
22. E. D. Zanotto and V. M. Fokin, Phil. Trans. R. Soc. Lond. A (2003) 361, 591-613
23. M. C. Weinberg, D. P. Birnie, V. A. Shneidman, J. Non-Cryst. Solids, 219 (1997) 89-99.
24. K. Matusita, S. Sakka, Bull. Inst. Chem. Res., Kyoto Univ., 59 (3) (1981) 159-171.
25. Y. Q. Gao, W. Wang, J. Non-Cryst. Solids, 81, 1986, 129-134.
26. S. Vyazovkin, K. Chrissafis, M. L. Di Lorenzo, N. Koga, M. Pijolat, B. Roduit, N. Sbirrazzuoli, J. J. Sunol, Thermochim. Acta, 520 (2011) 1-19.
27. S. Vyazovkin, New J. Chem., 24 (2000) 913-917.
28. A. T. W. Kempen, F. Sommer, E. J. Mittemeijer**,** Acta Mater., 50 (2002) 1319-1329.
29. F. Liu, C. Yang, G. Yang, Y. Zhou, Acta Mater., 55 (2007) 5255-5267.
30. A. A. Elabbar, M. Abu El-Oyoun, A.A. Abu-Sehly, S.N. Alamri, J. Phys. Chem. Solids, 69 (2008) 2527-2530.
31. B. Janković, M. Marinović-Cincović, M. Dramićanin, J. Phys. Chem. Solids, 85 (2015) 160-172.
32. J. Malek, Thermochim. Acta, 355 (2000) 239-253.
33. A. A. Abu-Sehly, M. Abu El-Oyoun, A.A. Elabbar, Thermochim. Acta, 472 (2008) 25-30.
34. F. Liu, F. Sommer, E. J. Mittemeijer, Acta Mater., 52 (2004) 3207-3216.
35. A. A. Abu-Sehly, A. A. Elabbar, Physica B, 390 (2007) 196-202.
36. A. A. Joraid, Thermochim. Acta, 456 (2007) 1-6.

37. A. M. Rodrigues, J. L. Narváez-Semanate, A. A. Cabral, A. C. M. Rodrigues, Mat. Res., 16 (4) (2013) 811-816.
38. A. M. Cruz, E. B. Ferreira, A. C. M. Rodrigues, J. Non-Cryst. Solids, 355 (2009) 2295-2301.

***Садржај**: Испитивана је кристализациона кинетика $22.5Li_2O•10Al_2O_3•30GeO_2•37.5P_2O_5$ (мол%) стакла под неизотермским условима коришћењем диференцијално термичке анализе (ДТА). Испитивања су извршена проучавањем кристалитационог пика T_{p1} фазе $LiGe_2(PO_4)_3$ у стаклу. Енергија активације (E_a) одређена је коришћењем различитих изокинетичких метода. Зависност E_a од степена кристализације (α) испитана је коришћењем KAS и WFO методе. Показано је да E_a варирара са степеном кристализације, а да је трансформација стакло/кристал комплексан процес који укључује различите механизме нуклеације и раста кристала.*

***Кључне речи**: литијум-германатнофосфатно стакло, кристализациона кинетика, ДТА, нуклеација.*